SOME RESULTS OF THE CRYOGENIC INFRARED SPECTROMETERS AND TELESCOPES FOR THE ATMOSPHERE (CRISTA) EXPERIMENT

M. Riese, R. Spang, J. Oberheide, G. Lehmacher, P. Preusse, and D. Offermann

Physics Department, University of Wuppertal, Gauss-Str. 20, D-42119 Wuppertal, Germany,
E-mail: riese@wpos2.physik.uni-wuppertal.de; Tel: +49 202 4392779; Fax: +49 202 2680

ABSTRACT

The CRISTA experiment aboard the Shuttle Pallet Satellite (SPAS) was flown on the Space Shuttle missions STS 66 (November 94) and STS 85 (August 97). During both missions atmospheric temperatures and trace gases mixing ratios were measured with unprecedented spatial resolution from a 300 km, 57° inclination orbit. This paper discusses validation measurements performed during CRISTA 2 as well as some of the results of CRISTA 1 [see also Refs. 1,2,3,4,5,6,32].

INSTRUMENT DESCRIPTION

CRISTA is a limb-scanning instrument, which measures global distributions of thermal emissions (4 - 71 μm) of trace gases and aerosols. The instrument is mounted on the reusable ASTRO-SPAS platform, which is released from the Shuttle and operates at a distance of 50 - 100 km behind it. The platform also houses the Middle Atmosphere High Resolution Spectrograph Investigation (MAHRSI) instrument, which performs UV measurements of OH and NO in the middle atmosphere [Ref. 7].

For improved horizontal resolution (typically 6° x 3°) CRISTA uses three telescopes that sense the atmosphere at angles 18° apart (see Figure 1). The optics and the infrared detectors are cooled by cryogenic helium. This results in high sensitivity of the detectors, and consequently, high measuring speed and high spatial resolution. Altitude scans of atmospheric emissions are performed by tiltable telescope mirrors. The incoming limb radiance is analyzed by four grating spectrometers with a spectral resolution of about 500. A detailed description of the instruments, tests and calibrations, and measured trace gases, is given by Offermann et al. [Ref. 1]. The CRISTA data processing and atmospheric temperature and trace gas retrieval are described by Riese et al. [Ref. 2].

VALIDATION MEASUREMENTS

Major elements of the two CRISTA missions were correlative measurements from ground based systems, balloons, rockets, and other satellite instruments [Ref. 8]. During the second mission the manuever capabilities of the CRISTA-SPAS satellite were used to point the viewing direction of CRISTA at selected validation sites. The pointing maneuvers worked flawlessly. Average minimal miss distances of about 30 km were achieved.

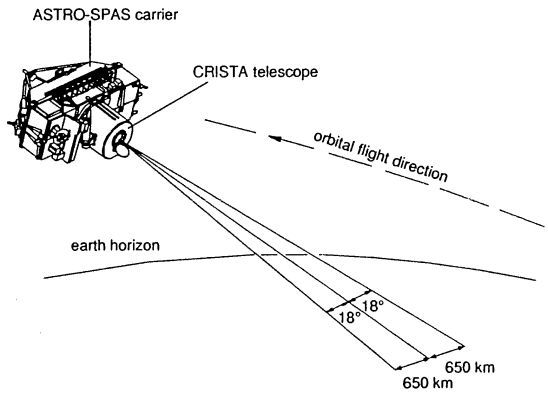

Figure 1: CRISTA measurement configuration during the second mission

An example of three consecutive orbits during CRISTA 2, including a validation orbit, is given in Figure 2. Shown are the footprints of profiles of a spectrometer (SCS) of the center telescope. The first and the third orbit are representative for the so-called ping-pong mode. In this mode the viewing direction was tilted northward in the northern parts of the orbits (and southward in the southern parts). This way, the latitudinal coverage of the measurements was extended to 74° N and 74° S. The second orbit, shown in Figure 2, is a validation orbit, where the viewing direction of the center telescope was directed towards the two main validation sites located at Wallops Islands, Virginia, US (37.9° N, 75.5° W), and Hohenpeisenberg, Germany (47.8° N, 11.0° E). The stations are indicated by the full diamonds in Figure 2.

The NASA/GSFC Flight Facility (WFF) was the main site for validation of CRISTA temperature measurements. Temperature validations are especially important, since atmospheric temperatures represent an essential input for the trace gas retrieval of CRISTA [Ref. 2]. For this reason, falling sphere

Proceedings 14th ESA Symposium on European Rocket and Balloon Programmes and Related Research, Potsdam, Germany, 31 May - 3 June 1999, (ESA SP-437, September 1999)

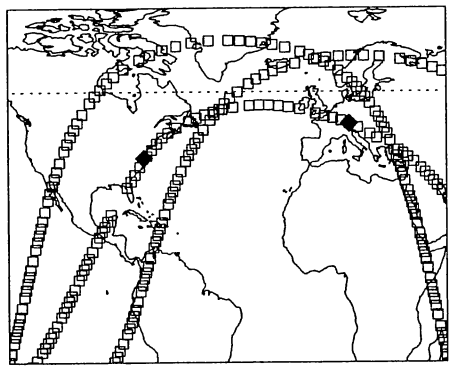

Figure 2: Footprints of the CRISTA SCS spectrometer (open squares) for three subsequent orbits. The second orbit is a validation orbit with CRISTA pointing at Wallops Island and Hohenpeissenberg (full diamonds). A dotted line is drawn at 57° N indicating the orbit inclination.

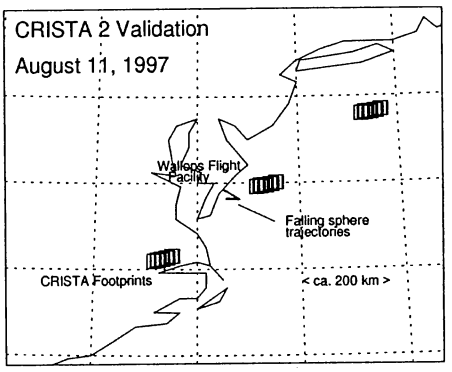

Figure 3: Details of the validation orbit on August 11, 1997. CRISTA footprints (open squares) are shown for three subsequent profiles measured by the SCL spectrometer. The horizontal projection of the trajectories of two falling spheres is also shown (V shaped line).

and data sonde launches were coordinated to obtain minimal miss time and minimal miss distance with respect to the CRISTA measurements. Falling spheres were launched in pairs within a few minutes to obtain coincident measurements at two different altitudes.

A close-up of the region around NASA/GSFC Wallops Flight Facility (WFF) is depicted in Figure 3. Shown is the location of the measurement points (center telescope) of three adjacent CRISTA vertical profiles of the validation orbit. The profiles are separated by about 290 km. The small V shaped line originating from the coast represents the trajectories of two falling spheres launched from WFF. Since the width of the horizontal weighting function of the limb-viewing method is on the order of 300 km, the CRISTA profile closest to WWF can be considered as zero miss distance profile.

The temperature profiles for both falling spheres and the zero miss distance profile are shown in Figure 4. The falling sphere profiles show a temperature inversion between 65-70 km. They agree with each other within the estimated statistical error of about 3-4 K at these altitudes [Ref. 9, 10]. However, the data suggest relatively high variability, especially in the vicinity of the temperature inversion. This variability is remarkable, when considering that the temperatures were measured within 5 minutes.

CRISTA temperatures agree well with the falling sphere observations. The inversion layer clearly shows up in the CRISTA profile suggesting that the horizontal extent of this feature must have been at least on the order of the horizontal weighting function of CRISTA. The neighboring CRISTA profiles (not shown) agree well below 60 km, but show larger temperature deviations in the dynamically disturbed region of the inversion.

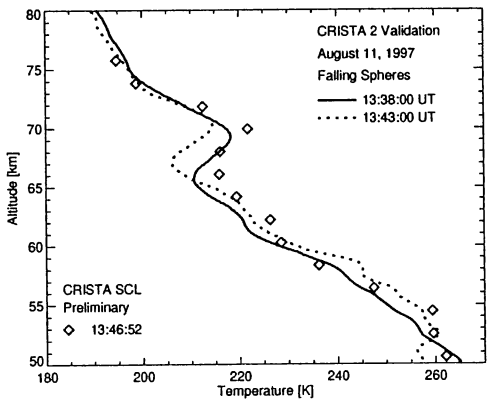

Figure 4: Figure 4 of Lehmacher et al. [Ref. 8]. Temperature profiles of two falling spheres (solid and dotted lines) and the zero miss distance CRISTA SCL temperature profile (diamonds). Note that CRISTA temperatures are preliminary (non-version) data.

THERMAL TIDES

CRISTA temperature observations exhibit signifi-

cant tidal signatures [Ref. 4]. Important tidal features are, for example, diurnal migrating solar tides generated by periodic absorptions of solar radiance, primarily UV absorptions of ozone in the stratopause region and IR absorptions of H_2O in the troposphere. Migrating tidal waves follow the westward movement of the sun. Since the zonal wavenumber is equal to the number of oscillations per day, the phase at a given latitude only depends on the local solar time (LST).

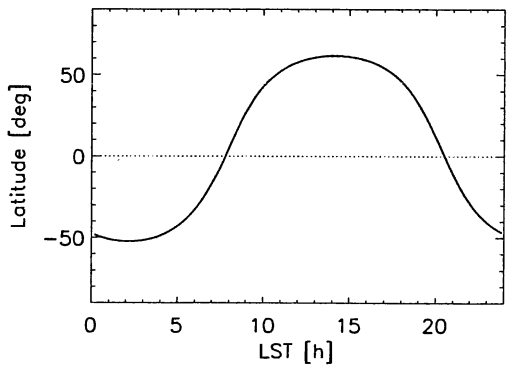

Figure 5: Local solar time distribution (LST) of the center telescope at points around an orbit for November 9, 1994. The LST shifts 22 minutes per day. In the equatorial region, measurements at the ascending portion of the orbit are performed at 8 LST. Measurements at the descending portion are performed at 20 LST.

Tidal waves have been studied since more than 30 years using ground based and satellite borne wind and temperature measurements. Recently, the amount of wind data significantly increased due to observations performed by the Wind Imaging Interferometer (WINDII) [Ref. 11] and the High Resolution Doppler Imager (HRDI) [Ref. 12] on the Upper Atmosphere Research Satellite (UARS). First global analyses of tidal signatures in atmospheric temperature fields were obtained from measurements of the Limb Infrared Monitor of the Stratosphere instrument (LIMS) on the Nimbus 7 satellite [Ref. 13]. Hitchman and Leovy [Ref. 14] report structures in day/night temperature differences consistent with the (1,1) mode of the migrating diurnal tide, i.e. maximum amplitudes at equatorial and middle latitudes.

CRISTA observations provide an opportunity to examine the structure of tidal waves throughout the middle atmosphere with extended vertical coverage and improved accuracy at upper mesospheric heights. Although the LST variation during the first mission is too small for a comprehensive spectral analysis, some tidal features are captured due to LST differences between the ascending and the descending portion of each orbit. These differences are of the order of 12 hours for most of the latitudinal band covered by CRISTA 1 (see Figure 5).

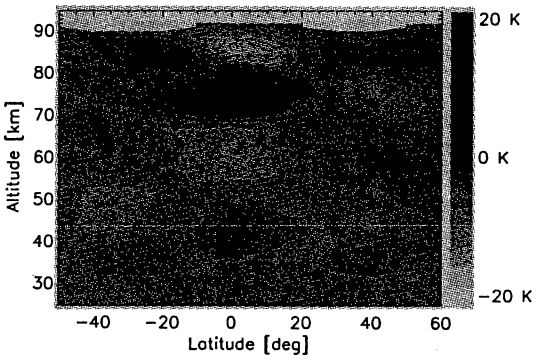

Figure 6: Latitude/height plot of zonal mean temperature differences for November 9, 1994. The differences were calculated from zonal mean temperatures obtained from observations during the ascending and descending part of each orbit. Positive values are indicated by solid isolines. Negative values are represented by dashed lines. Version 3 data of CRISTA 1 were used.

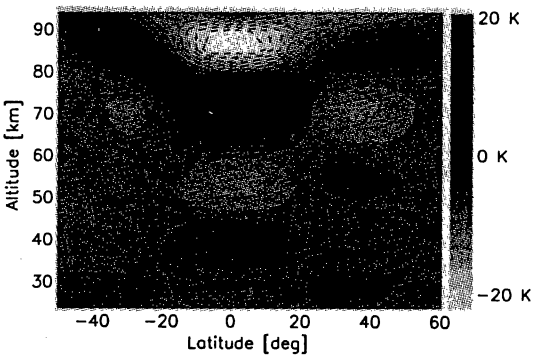

Figure 7: Same as Figure 6 but zonal mean temperature differences were calculated from the Global Scale Wave Model of Hagan et al. [Ref. 16] for equinox conditions.

Figure 6 shows zonally averaged temperature differences (ascending minus descending) for Nov. 9, 1994. The most apparent feature is the vertical pattern of alternating temperature minima and maxima at the equator and at middle latitudes. This pattern is characteristic of the (1,1) Hough mode and repre-

sentative for the first symmetric propagating diurnal tide [Ref. 15].

The main tidal structure observed by CRISTA is also present in a corresponding distribution of the Global Scale Wave Model (GSWM) [Ref. 16] calculated for the same LST (Figure 7) but equinox conditions. Temperature differences observed by CRISTA and simulated by GWSM are in good qualitative and quantitative agreement. The most important difference concerns the vertical wavelengths. The simulated wavelengths are somewhat smaller in the stratosphere and somewhat larger in the mesosphere. Ward et al. [Ref. 4] derived associated equivalent displacement heights of air parcels driven by the tidal motion. It is planned to validate these displacement heights [see also Ref. 17] by means of CRISTA trace constituent fields.

GRAVITY WAVES

Most observational studies of gravity waves (GW) are based on ground-based observations from a limited number of locations (e. g. [Ref. 18]). More recently, global data sets obtained from satellite measurements have been used for GW studies [Ref. 19, 20]. CRISTA data allow analysis of gravity waves with vertical wavelengths larger than about 4 km [Ref. 21]. For example, Preusse et al. [Ref. 22] discuss temperature profiles measured in the lee of the Andes in terms of mountain waves. The southern tip of South America is found to be a region of very high GW activity in the lower stratosphere during the CRISTA 1 measurement period.

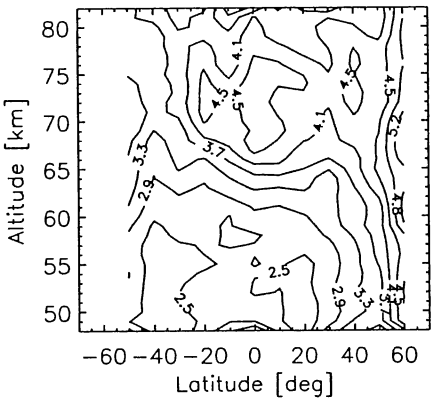

Figure 8: Zonal mean amplitudes of gravity waves (in Kelvin) derived from CRISTA 1 temperature data (V3).

Figure 8 shows zonal mean amplitudes of gravity waves (K) with vertical wavelengths between 6 and 12 km for CRISTA 1. Largest amplitudes occur northward of 50° N. The local maximum at equatorial latitudes and 75 km altitude possibly indicates a non-linear interaction of gravity waves and the highly excited tidal wave (see Figure 6).

TRACE GAS MODELING

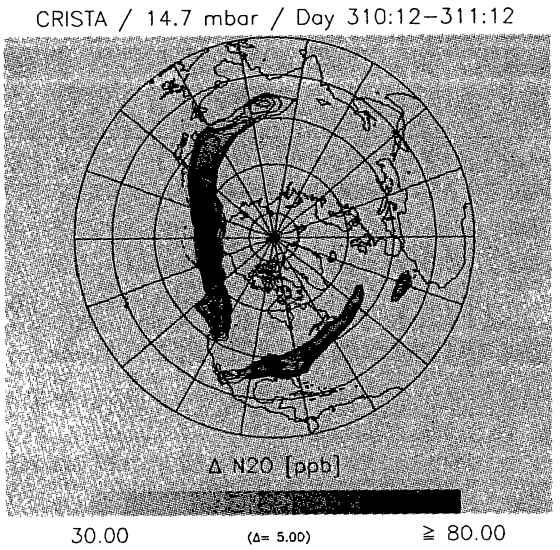

Figure 9: Extrusions of tropical air measured by CRISTA 1. Results are shown for detrended N_2O mixing ratios (V1). (For details see text.)

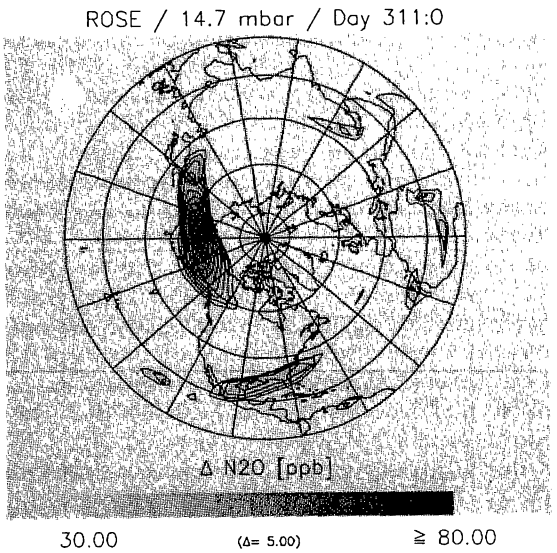

Figure 10: Same as Figure 9 but model results.

The first flight was performed in early November 1994 during a period of disturbed dynamical conditions characterized by relatively large wave activity and associated exchange of tropical and extra-

tropical air. As a result, numerous small and medium scale structures were present in the trace gas distributions measured by CRISTA. The detailed structure of the constituent distributions has been simulated with the NCAR ROSE model [Ref. 3].

The three-dimensional ROSE model has been used for several previous studies of the middle atmosphere (see Refs. [23,24,25,26]). In these studies, the model calculates "on line" the dynamical variables of the atmosphere (e. g. wind and temperature above 300 mbar). In the present case, the model version is driven "off line" by analyzed winds and temperatures provided by the UK Meteorological Office (UKMO) [see also Ref. 27].

The ROSE model was initialized on November 1, 1994, based on correlation parameters describing the relationship between UKMO potential vorticity (PV) fields and long-lived tracers measured by CRISTA. No information about structures in the constituent fields observed by CRISTA enters the initialization. More details are given by Riese et al. [Ref. 3].

A comparison of measured and modeled structures in the northern hemispheric N_2O distribution (14.7 mbar) is shown in Figures 9 and 10 for November 7, 1994 (Day 311). To emphazise the synoptic structures, the N_2O values have been "detrended" by subtracting zonal mean values at each latitude. Figures 9 and 10 only show values, which are at least 30 ppb higher than associated zonal mean mixing ratios.

Two pronounced tropical extrusions can be seen in both CRISTA observation and simulation. However, the strengths of these extrusions is somewhat underestimated in the simulation. In the tropics and subtropics, the model results exhibit large medium scale variability, which does not exist in the measured distribution (not shown here; see also Ref. 28). Implications for horizontal trace gas eddy transport are discussed by Riese et al., 1999 [Ref. 3].

CLOUD MEASUREMENTS

For the detection of clouds and high aerosol loadings a cloud index was tentatively defined by means of the intensity ratio of the CO_2 Q-branch at 792 cm^{-1} and an aerosol channel at 833 cm^{-1} [Ref. 29]. A ratio of two or smaller was considered to be indicative of a cloud.

Figure 11 shows the resulting cloud occurrence frequency at 18 km for November 8, 1994. The distribution resembles a SAGE II climatology of subvisible clouds [Figure 12; Ref. 30] to a large degree, e. g. large cloud rates occur in the equator region centered around the Amazon, Congo, and Indonesia. These are areas of strong upwelling and deep convection. In addition, the CRISTA distribution exhibits an area of high cloudiness centered around the date line consistent with convection patterns associated with an El Nino event.

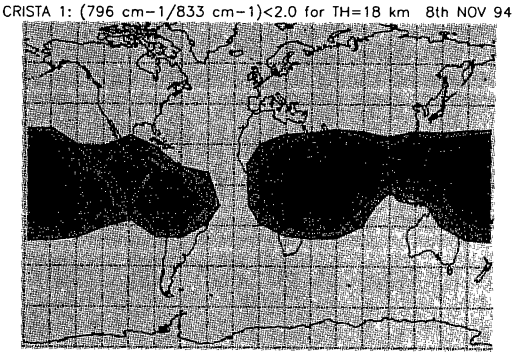

Figure 11: CRISTA 1 cloud frequencies on Nov. 8, 1994 at 18 km altitude. The numbers indicate the fraction of measurements influenced by clouds.

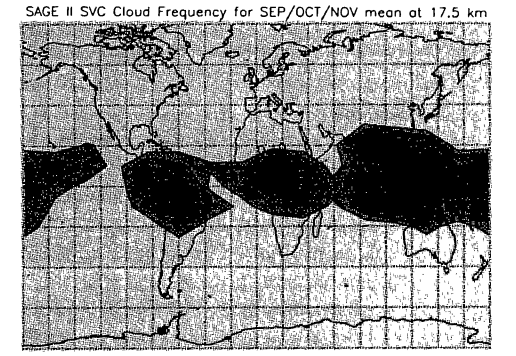

Figure 12: SAGE II climatology for subvisible clouds (Sep/Oct/Nov average).

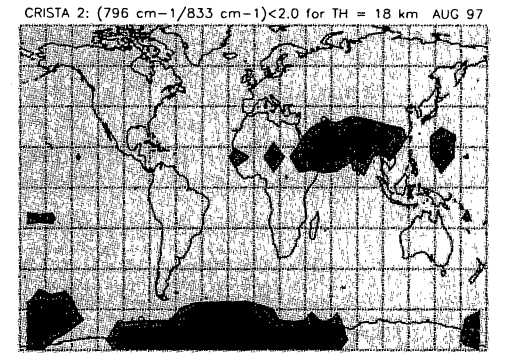

Figure 13: Figure 1c of Offermann and Spang [Ref. 29]. CRISTA 2 cloud frequencies. Shown are mean values for a measuring period of one week in early August 1997.

Cloud frequencies of the second CRISTA mission (August 97) are shown in Figure 13. In the tropics, cloud frequencies are much smaller than during

CRISTA 1. Thus, seasonal variations clearly show up. In addition, considerable cloud cover is seen over Antarctica, most likely due to PSC type II (ice) particles. The PSCs are located at altitudes around 24 km. However, they also influence the measurements at 18 km tangent height [Figure 13] due to the limb viewing geometry [Ref. 2]. The spatial and temporal structures of these clouds are currently studied as well as the influence on trace gas distributions measured by CRISTA and GOME [Ref. 31].

OTHER RESULTS AND OUTLOOK

CRISTA 1 temperature values near the stratopause show stacked pertubations with short vertical scales (10 km). The structures are consistent with low latitude circulation responding to inertial instability. Concentrations of two analysed species (ozone and methane) show pertubations consistent with the predicted response to an inertially unstable circulation, either through transport (methane) or photochemical changes (ozone). A detailed description and interpretation of these observations is given by Smith and Riese [Ref. 32]

For quantitative comparisons of trace gas transport in the ROSE model and trace gas transport associated with the measurements, CRISTA (Level 2) data have been assimilated into the model by using a sequential technique. The trace gas assimilation system interpolates the measured distributions of long-lived tracers onto the model grid and yields synoptic fields that are consistent with the CRISTA measurements, at each time step of the model (20 min). Since wind and temperature data are available on the same synoptic grids, detailed transport and trace gas budget studies become feasible [Ref. 3].

Recently, an assimilation scheme for chemically active species (NO_2, N_2O_5, HNO_3, $ClONO_2$, ...) has been developed and implemented. This system allows detailed photochemical analyses. In a first study, the influence of heterogeneous reactions on the partitioning ratios of NO_y members has been analysed in detail.

REFERENCES

1. Offermann D et al. 1999, Cryogenic Infrared Spectrometers and Telescopes for the Atmosphere (CRISTA) experiment and middle atmosphere variability, *J. Geophys. Res.*, in press.

2. Riese M et al. 1999, Cryogenic Infrared Spectrometers and Telescopes for the Atmosphere (CRISTA) data processing and atmospheric temperature and trace gas retrieval, *J. Geophys. Res.*, in press.

3. Riese M et al. 1999, Three-dimensional simulation of stratospheric trace gas distributions measured by CRISTA, *J. Geophys. Res.*, in press.

4. Ward W E et al. 1999, Tidal signatures in temperature data from the CRISTA I mission, *J. Geophys. Res.*, in press.

5. Bacmeister J et al. 1999, Intercomparison of satellite and aircraft observations of ozone, CFC-11, and NO_y using trajectory mapping, *J. Geophys. Res.*, in press.

6. Kouker W et al. 1999, Streamers observed by the CRISTA experiment and simulated in the KASIMA model, *J. Geophys. Res.*, in press.

7. Conway R et al. 1999, Middle atmosphere high resolution spectrograph investigation , *J. Geophys. Res.*, in press.

8. Lehmacher G A et al. 1999, Zero miss time and zero miss distance experiments for validation of CRISTA 2 temperatures, submitted to *Adv. Space Res.*

9. Lübken F J et al. 1994, Intercomparison of density and temperature profiles obtained by lidar, ionization gauges, falling spheres, datasondes, and radiosondes during the DYANA campaign, *J. Atmos. Terr. Phys.*, 56, pp. 1969–1984.

10. Schmidlin F J et al. 1991, The inflatable sphere: A technique for the accurate measurement of middle atmosphere temperature, *J. Geophys. Res.*, 96, pp. 22673–22682.

11. Shepard G G et al. 1993, WINDII, the wind imaging interferometer on the Upper Atmosphere Research Satellite, *J. Geophys. Res.*, 98, pp. 10725–10750.

12. Hays P B et al. 1991, The High–Resolution Doppler Imager on the Upper Research Satellite, *J. Geophys. Res.*, 98, pp. 10713–10723.

13. Gille J C and J M Russell III 1984, The Limb Infrared Monitor of the Stratosphere: Experiment description, performance, and results, *J. Geophys. Res.*, 89, pp. 5125–5140.

14. Hitchman M H and Leovy C B 1985, Diurnal tide in the equatorial middle atmosphere as seen in LIMS temperatures, *J. Atmos. Sci.*, 42, pp. 557–561.

15. Forbes J M 1982, Atmospheric tides 1. Model description and results for the solar diurnal component, *J. Geophys. Res.*, 87, pp. 5222–5240.

16. Hagan M E et al. 1995, On modeling migrating solar tides, *Geophys. Res. Lett.*, 22, pp. 893–896.

17. Ehhalt D H et al. 1984, On the temporal variance of stratospheric trace gas concentrations, *J. Atmos. Chem.*, 1, pp. 27–54.

18. Eckermann S D et al. 1995, Gravity wave and equatorial wave morphology of the stratosphere derived from long-term rocket soundings, *Q. J. R. Meteorol. Soc.*, 121, pp. 146–186.

19. Fetzer E J and Gille J C 1994, Gravity wave variance in LIMS temperatures, Part I: Variability and comparisons with background winds, *J. Atmos. Sci.*, 51, pp. 2461–2483.

20. Wu D L and J W Waters 1996, Satellite observation of atmospheric variance: A possible indication of gravity waves, *Geophys. Res. Lett.*, 23, pp. 3631–3634.

21. Preusse P et al. 1999, Evidence for gravity waves in CRISTA temperatures, accepted for publication in *Adv. Space Research,*

22. Preusse P et al., Mountain lee waves over South America - a case study on the sensitivity to spatial short scales, to appear in *Proceedings of European workshop on mesoscale processes in the stratosphere: Their effect on stratospheric chemistry and microphysics*, Bad Toelz, Germany, 8-11 November, 1998.

23. Rose K 1983, On the influence of nonlinear wave-wave interactions in a 3-d primitive equation model for sudden stratospheric warmings, *Beitr. Phys. Atmosph.*, 19, pp. 14–41.

24. Rose K and G Brasseur 1989, A three-dimensional model of chemically active trace species in the middle atmosphere during disturbed winter conditions, *J. Geophys. Res.*,96, pp. 16,387–16,403.

25. Granier C and G Brasseur 1991, Ozone and other trace gases in the Arctic and Antarctic regions: Three-dimensional model simulations, *J. Geophys. Res.*, 96, pp. 2995–3011.

26. Smith A K 1996, Numerical simulations of global variations of temperature, ozone, and trace species in the stratosphere, *J. Geophys. Res.*,100, pp. 1253–1269.

27. Lefèvre F et al. 1994, Chemistry of the 1991-1992 stratospheric winter: Three-dimensional model simulations, *J. Geophys. Res.*, 99, pp. 8,183–8,195.

28. Kindler T P et al. 1998, An evaluation using ^{14}C and N_2O simulations of three-dimensional transport driven by United Kingdom Meteorological Office and Goddard Space Flight Center assimilated winds, *J. Geophys. Res.*, 103, 10,827–10,847.

29. Offermann D and R Spang 1999, Detection of stratospheric clouds in Antarctica and in the tropics by CRISTA, to appear in *Proceedings of European workshop on mesoscale processes in the stratosphere: Their effect on stratospheric chemistry and microphysics*, Bad Toelz, Germany, 8-11 November, 1998.

30. Wang P H et al. 1996, A 6-year climatology of cloud occurence frequency from SAGE II observations (1985–1990), *J. Geophys. Res.*,101, pp. 29407–29429.

31. Hild L et al., 1999, A study of PSC activation of chlorine during the austral winter 1997, to appear in *Proceedings of the European symposium on atmospheric measurements from space,* Noordwijk, The Netherlands, 20-22 Januar, 1999.

32. Smith A K and M Riese 1999, CRISTA observations of tracer transport by inertially unstable circulations, submitted to *J. Geophys. Res.* in press.